Chemistry and Physics of Lipids 158 (2009) 10–15

Contents lists available at ScienceDirect

Chemistry and Physics of Lipids

journal homepage: www.elsevier.com/locate/chemphyslip

# Unit cell volume and liquid-phase immiscibility in oleate–stearate lipid mixtures

Walter F. Schmidt[a,*], Swati Mookherji[a], Michael A. Crawford[b]

[a] United States Department of Agriculture (USDA), Beltsville Agricultural Research Service (BARC), Agricultural Research Service (ARS), Beltsville, MD 20705, United States
[b] Institute of Brain Chemistry and Human Nutrition, University of North London, UK

ARTICLE INFO

*Article history:*
Received 14 May 2008
Received in revised form 1 December 2008
Accepted 8 December 2008
Available online 25 December 2008

*Keywords:*
Cubic unit cell volume
Oleic acid
Methyl oleate
Stearic acid
Immiscible lipid phases
Cloud point
Stoichiometry

ABSTRACT

The structural basis of immiscibility of stearic acid (SA) in two unsaturated lipids at room temperature was examined. A 5% SA mixture in octadec-9-enoic acid (OA) is cloudy; a 5% SA solution in the methyl ester of OA (MeOA) is fully miscible. At 10% SA in MeOA, a clear and immiscible phase formed. The composition of this immiscible phase however was not 10% SA, but 25% SA. Adding additional SA altered the amount of the second phase, not its stoichiometry. Molecular mechanics explains the molecular basis for the ratio of saturated and unsaturated lipids in the different phases. Packing order of lipids within a unit volume explains the discrete lipid composition ratio forming each of the observed miscible and immiscible phases. The smallest unit cell volume that explains the observed stoichiometry is a cube (not a sphere).

Published by Elsevier Ireland Ltd

## 1. Introduction

Natural lipids appear to pack more efficiently than synthetic lipids (Li et al., 2003; Broadhurst et al., 2004). Order versus disorder among the double bond regions of polyunsaturated lipids in natural matrices is experimentally difficult to access structurally because each inter- and intra-molecular interactions are not easily differentiated. Understanding the packing among less complicated mixtures of lipids can be the access to a structural basis for lipid packing.

Disorder in packing among lipids would predict saturated and unsaturated lipids would innately be fully miscible. Yet, lipid immiscibility is clearly evident in the cloud point (CP) present in biodiesel production. The composition of biodiesel fuel is a mixture of saturated and unsaturated fatty acid methyl esters (FAME).

The transesterification of the triacylglycerols of vegetable and/or animal origin produce methyl esters which are used as biofuel. CP is the temperature at which diesel lipids become cloudy. A model for CP prediction in biodiesel fuel has been established (Imahara et al., 2006). The study found that CP of methyl esters in biodiesel could be described using solid–liquid equilibria and assuming that only one ester component is crystallized at a CP. However, neither the chemical composition which enables nucleation, nor the composition of the "crystalline" phase which formed was chemically analyzed.

Octadec-9-enoic acid (OA) and octadecanoic acid (SA) are two major FAME components in biofuel. Spectroscopic data found molecular order in OA is present at room temperature, but absent at higher temperatures (Iwahashi et al., 1991). Molecular order in OA could be the precursor of immiscibility in mixtures. Again, disorder in packing among lipids predicts binary mixtures of SA and OA would be totally miscible.

A study of solid–liquid-phase interactions of OA and SA by differential scan calorimetry (DSC), and Fourier transform infrared spectroscopy (FT-IR) indicated that the two fatty acid species are completely immiscible in a solid phase and are miscible in a liquid phase; their miscibility was related to the formation of OA and SA dimers (Inoue et al., 2004; Iwahashi et al.,2005). This explanation however is incomplete because OA/OA and SA/SA as well as OA/SA can form dimer pairs, and because dimer formation can just as well occur in forming miscible as immiscible phases.

The solubility at multiple temperatures of SA in structurally diverse organic solvents was recently investigated (Schmidt et al., 2006). The ratio of SA to solvent has a precise temperature dependent stoichiometry. 25 SA molecules spatially pack the space of a cubic volume with 1D equal to the length of a straight SA molecule. In saturated solutions of SA, near the melting point of SA, half the volume of the cube is SA and half the volume is SA. The solvents form a monolayer around SA replacing half the columns of the cube.

* Corresponding author. Tel.: +1 301 504 6765.
*E-mail address:* walter.schmidt@ars.usda.gov (W.F. Schmidt).

0009-3084/$ – see front matter. Published by Elsevier Ireland Ltd
doi:10.1016/j.chemphyslip.2008.12.005

The model of solubility could also apply to the miscibility of saturated lipids "dissolved" in mono-unsaturated lipids. Structurally OA and its methyl ester (MeOA) are similar in molecular size and shape. Since only OA can readily form –COOH HOOC dimers with –COOH from SA, the effect of dimer formation on SA miscibility in OA and MeOA can be tested.

Raman microscopy imaging was used to identify the potential compositional uniformity and/or heterogeneity within each phase. NMR spectroscopy was used to confirm the chemical composition both single "pure" phase, and of the immiscible second phase. Molecular mechanics was used to model the packing of lipids at the experimentally measured stoichiometry within unit cell phase volumes.

## 2. Experimental

### 2.1. Phase compositions

Samples of highly pure (>99.9%) OA, SA, and MeOA were obtained from Sigma–Aldrich. One gram of OA and of MeOA was weighed into separate glass scintillation vial and 10 mg SA was added in to each vial. Vials were heated in a microwave oven until all solids dissolved. The mixture was slowly allowed to cool to the room temperature (22 °C). The solution then was allowed to equilibrate at the constant temperature for 24–48 h. An additional 10 mg of solid SA was added to the vial, and again the vial was heated in a microwave oven until all solids dissolved, and then allowed to cool slowly. When uncertainty existed about the formation of a second phase, sample would be reheated without adding additional SA.

The number fraction of two components in a lipid mixture is the mole fraction of each component. The ratio of SA to OA was measured in weight % and converted to mole %: 282.5 g/mole OA = 284.5 g/mole SA = 294.5 g/mole MeOA.

### 2.2. Raman spectroscopy and imaging microscopy

Samples (ca. 1–10 mg) were placed on an aluminum tape lined glass slide. Raman spectra were collected using a LabRam Aramis confocal Raman microscope (Horiba Jobin Yvon, Edison, New Jersey) with a 10×, 50×, and 100× objectives. The spectra were collected over the range of 200–4000 $cm^{-1}$ Raman shift using a HeNe laser (633 nm) for excitation. The confocal hole, and slit aperture were 500 μm and 100 μm, respectively. Maps were generated using a grating of 1200 g/mm, exposure time of 5 s with 20 accumulations per data point. In maps, spectral range was reduced to 600–1800 $cm^{-1}$.

For Raman imaging, and map of mixtures, a microscopic field of view was selected to include two lipid phases simultaneously. In map processing of mixtures following frequency ranges were selected: 1035–1162 $cm^{-1}$ (for C—C group), 1403–1459 $cm^{-1}$ (for C—H group), and 1476–1772 $cm^{-1}$ (for C=C and C=O group). On the region chosen for mapping, the program plots the localized distribution and intensity of these specific peaks.

### 2.3. NMR spectroscopy

The NMR spectra were recorded using an Eft-90 spectrometer (Anasazi Instruments, Indianapolis, IN). Solutions (50 mg/ml) of single and mixed lipids were with $CDCl_3$ in NMR tubes, and proton spectra were acquired with a spectral width of 900 Hz and 4 K data points. The chemical shifts are reported relative to reference standard tetramethylsilane, and the fraction composition of each physically distinct phase was determined by integration. Integration was confirmed by spectral subtraction.

### 2.4. Molecular mechanics

The chemical structure of individual lipid molecules was generated on HyperChem 8.0 (Gainesville, FL). The packing among lipid molecules was optimized using MM + force fields (Zhdanov et al., 2003). The conjugate gradient (Fletcher-Reeves) method was used to energy minimize distances among lipid molecules. Convergence condition limits were a RMS gradient of 0.01 kcal/Å mol. The packing among the lipids was the smallest cubical molecular volume in which stoichiometry could maintain the macroscopic mole ratios determined experimentally.

## 3. Results and discussion

### 3.1. Phase separations

Immiscibility and phase separation at room temperature (22 ± 2 °C) occurred upon adding excess SA to either of the unsaturated lipids. Adding up to 2% SA to OA resulted in a clear liquid phase. At 5% SA, the lipid became cloudy. Increasing the concentration of SA further increased the fraction of the sample that was cloudy and the resulting lipid became viscous. The mass and volume of the second phase that formed however was obviously greater than the mass and volume of SA which had been added.

A clear liquid phase occurred in adding up to 5% SA to MeOA. Addition of 10% SA to MeOA resulted in a solution that remained clear for several days at 22 ± 2 °C; a soft crystalline lipid phase then formed that was stable indefinitely. Increasing the SA concentration to 30% resulted in a cloudy, macroscopically amorphous phase. Again the mass and volume of solid material which formed was clearly in excess of the amount of SA added.

A possible explanation for the dissimilar physical properties between the two mixtures is that OA and SA are free fatty acids which can form dimers. MeOA as an ester is satirically hindered from forming dimers with SA. Three sets of dimers could be forming from SA and OA: SA/SA, SA/OA, and OA/OA. Assuming each free fatty acid pair is equally likely to form, when more OA than SA molecules are present, OA/OA dimer interaction would predominate, and SA/OA dimers would form more often than SA/SA dimers.

A dimer formation hypothesis in lipids is a 1D explanation. Even in 1D only when two molecules are approaching each other head to head (—COOH to HOOC—) can a dimer form. Foot to foot (terminal —$CH_3$ to $H_3C$—) or head to foot associations will not form a dimer. The number averaged associations which do not form dimers versus those that do are 1/4. In a 2D space in a vacuum, two molecules can approach each other at any angle from 0° to 360°. No dimer formation would occur if the —COOH group approached anywhere in the middle of the long molecule. In a 3D space, the number of other possible orientations by which two SA molecule could associate other than head–head and in a straight line far exceeds the 1/4 ratio estimated from a 1D experiment.

An entirely different set of explanations would be required to explain SA solubility in MeOA. In this case, only SA/SA dimer could readily form. Dimer formation would be far more likely in OA than in MeOA, yet empirically SA was more than twice as soluble in MeOA as in OA. Clearly dimer formation with SA does not account for this higher solubility in MeOA than in OA.

### 3.2. Raman spectroscopy, microscopy and mapping

The chemical structures of each component alone and in a binary mixture were identified using Raman spectroscopy (Table 1). Assignments are consistent with published frequencies (Socrates, 2001). Frequencies near 1092, 1118 and 1162 $cm^{-1}$ were markers for SA and not present in OA or MeOA. The C=C alkyl stretching frequencies near 1292 and 1646 $cm^{-1}$ and C—H stretching (i.e. in

**Table 1**
Assignment of Raman spectral frequency bands in pure SA. OA, and MeOA and in SA mixture with OA and MeOA 1st and 2nd phases are immiscible.

| Functional group | SA (pure) | OA (pure) | MeOA (pure) | 1st phase SA/OA | 2nd phase SA/OA | 1st phase SA/MeOA | 2nd phase SA/MeOA |
|---|---|---|---|---|---|---|---|
| C—C | 1050 | 1052 | 1051 | 1047 | 1049 | 1049 | 1050 |
| | | 1073 | 1072 | | | 1073 | |
| C—C | 1092 | | | 1090 | 1092 | 1092 | 1092 |
| | | 1105 | 1103 | | | | |
| | 118 | | | 1118 | 1118 | 1117 | |
| | 1162 | | | 1158 | 1162 | 1160 | 1159 |
| | | 1254 | 1256 | 1252 | | 1250 | 1252 |
| C=C | | 1292 | 1286 | 1290 | 1286 | 1288 | 1289 |
| C—H | 1431 | 1428 | 1427 | 1427 | 1427 | 1425 | 1427 |
| C—H | | 1449 | | 1449 | 1447 | 1449 | 1448 |
| C=C | | 1646 | 1643 | 1642 | 1645 | 1645 | 1644 |
| C=O | | | 1730 | | | 1732 | 1732 |
| C—H | 2717 | 2719 | 2721 | 2717 | 2715 | 2715 | 2715 |
| $CH_2$sym | 2837 | 2843 | 2843 | 2842 | 2841 | 2841 | 2845 |
| $CH_3$sym | 2873 | 2866 | 2866 | | 2873 | 2873 | 2873 |
| $CH_2$Osym | 2913 | | 2919 | 2919 | 2914 | | |
| CH | | 3000 | 3000 | 3000 | 2999 | 2999 | 3000 |

CH=CH) at 3000 $cm^{-1}$ were present in OA and MeOA and not in SA. The ester C=O stretching frequency near 1730 $cm^{-1}$ was present only when MeOA was present (Table 1).

Structurally, a COOH group is also present in both SA and OA. However, C=O stretching frequencies near 1730 $cm^{-1}$ were not observed in either of the two "pure" lipids nor in the mixtures containing both. An explanation for the absence of frequencies in the carbonyl range is that —COOH···HOOC— dimers are forming (Adar et al., 2003; Baeten et al., 1998; Socrates, p. 126). Since new peaks in the same range also did not appear in any of the phases containing mixtures of SA and OA, there is no evidence of a change in the amount or kind of dimer formation that had occurred in either phase as the mole ratio of SA/OA changed.

Unambiguously, and unexpectedly, unsaturated lipids were the primary component in each of the second immiscible phases. SA was the lesser mole fraction/volume component. The assay of both components in all four phases was performed using NMR spectroscopy (Section 3.3).

Presence of SA in both phases was evident from peaks at 1118 and 1162 $cm^{-1}$. The Raman spectra were from the solid/crystalline SA. The simplest explanation for this difference is the packing of SA at the molecular level in the matrix is also not identical to the packing in the solid state. The C=C alkyl stretching frequencies near 1292 and 1646 $cm^{-1}$ and the C—H stretching (i.e. in CH=CH) near 3000 $cm^{-1}$ were considerably more intense than the SA frequencies, consistent with SA as the minor component in the second phase.

A matrix effect was also detected in the packing of the unsaturated lipid component of the mixtures. The largest difference (1–4 $cm^{-1}$) between the frequencies of OA (and of MeOA) compared to the corresponding frequencies in biphasic mixtures was in the $CH_2$ sym stretching region. Strong peaks near 1105 and 1103 $cm^{-1}$ were not found in the binary mixtures and were present in the individual unsaturated lipid spectra. Although, some Raman spectral frequencies such as 1431 and 2717 $cm^{-1}$ in mixtures are not unambiguously assignable to the saturated and/or the unsaturated lipid component of the single component(s), the new frequencies present indicate packing among lipids are interdependent and different from that of the single components.

Raman mapping enabled spectra characterization of the two intact immiscible phases observed microscopically. The microscopic structure (Fig. 1A) is similar in shape to the map of the two-phase components (Fig. 1B). The uniformity in the white region (phase 2) was due to the homogeneity of SA (and of MeOA) in concentration in that physical morphological structure. The uniformity in the pink region (phase 1) was due the homogeneity of MeOA (and of SA) in concentration in that morphological phase. Although, microscopically and macroscopically dispersed, site-to-site, the composition in the mixture within microscopically similar regions internally was consistently uniform.

The scale of microscopic image was at lower magnification than the Raman map because at higher magnification the boundaries between the two phases were difficult to differentiate (due to refractive index changes). The *XY*-coordinates also were not identical between the image and the map because the second phase apparently moved several microns or slightly melted during mapping. The relative colors within and between sites however remained the consistent as long as both phases were simultaneously present.

Microscopically, the *in situ* shape of the second phase in SA in OA was composed of rough irregular surfaces on yellow spheres. SA in MeOA was composed of colorless layered soft crystals with a smooth orderly surface. Raman mapping demonstrated that the SA composition was homogeneous within each of the four phases. The immiscible second phase was just as uniform and regular at the molecular level as the "pure" liquid phase. Composition at the molecular level within each phase thus also had an interfacial effect at the microscopic level.

### 3.3. NMR spectroscopy

Quantitative $^1$H NMR is a straightforward routine analytical technique (Braun et al., 1998). When two chemically different lipid components are present together in the same solvent, each set of

**Table 2**
Chemical composition of SA in OA and SA in MeOA.

| | $m/(1-m)$ Phase 1 | $(1-m)$ Phase 1 | $m$ Phase 1 | $m/(1-m)$ Phase 2 | $(1-m)$ Phase 2 | $m$ Phase 2 |
|---|---|---|---|---|---|---|
| SA | 0.02 | | 0.02 | 0.05 | | 0.05 |
| OA | | 0.98 | | | 0.95 | |
| SA | 0.05 | | 0.05 | 0.33 | | 0.25 |
| MeOA | | 0.95 | | | 0.67 | |

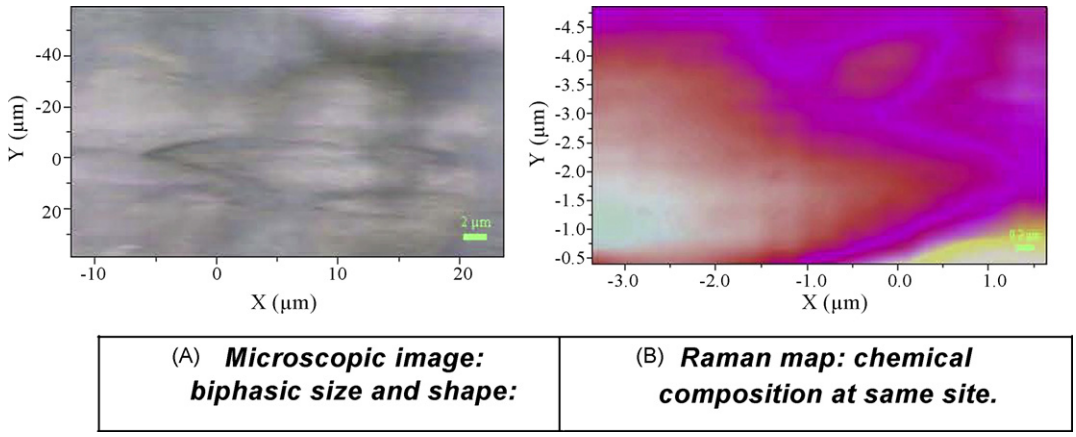


**Fig. 1.** Raman Mapping of Biphasic SA/MeOA lipid mixture. (A) Microscopic image of a clear, colorless soft crystalline phase surrounded by a clear liquid phase both of SA in MeOA. Small refractive index differences distinguish outlines of physical structures. (B) Raman map at the same site, enlarged. Uniformity of color within a region corresponds to uniformity of chemical composition. Contour plot lines occur in the microscopic structures that are not perfectly flat.

peaks is directly proportional to its mole fraction of the total concentration. The two proton peak area of the $-CH_2-COOH$ frequency (ca. 2.5 ppm) was used to quantify SA. The two proton peak area of the —CH=CH— frequency (ca. 5.1–6.1 ppm) was used to quantify the OA and MeOA component. The ratio of their integration equals the ratio of their mole fraction to each other in the mixture. Integration was confirmed by spectral subtraction.

The cloudiness of SA in OA (Phase 2) occurs when more than one molecule of SA does not fit into a space containing twenty OA molecules. In contrast, only a three molecules of MeOA are required to keep each SA molecule "dissolved." The model of lipids as spheres randomly bumping into each other an amorphous sea of lipids can never explain this difference in stoichiometry. Since the composition of the four phases have precise mole ratios, molecular order (i.e. packing) of lipids within unit cubic cell volumes must be present.

### 3.4. Molecular mechanics

Modeling lipid packing in a cubic unit cell volume has previously been described (Schmidt et al., 2006). The cubic phase volume is the smallest 3D molecular volume (24.8 $Å^3$) = 15,253 $Å^3$ that Table 2 explains the observed stoichiometry of binary mixtures of lipids: the value 24.8 Å is the length of one straight chain SA molecule. At any specific stoichiometry of solvents and SA, packing within the volume is effectively molecules at van der Waals distances from each other. The packing of OA within a unit cell could be similar. [*Cis*] polyunsaturated fatty acids including DHA are U-shaped molecules (Broadhurst et al., 2004) and may pack more efficiently than polyunsaturated fats with fewer *cis* bonds.

X-ray diffraction confirmed the anisotropic molecular order in liquid OA at room temperature and identified two distinct molecular dimensions present in this structure: 17.4 Å and 4.5 Å (Iwahashi et al., 1991). No three-dimensional picture of this structure, however, had been postulated. Molecular order has also been examined in shorter chain alcohols. Calculating scattering intensities from Monte Carlo simulation results and validation with SAXS data demonstrated that the structural properties of shorter chain alcohols have a dynamic molecular size component (Tomsic et al., 2007). In this investigation, SA and OA and MeOA are comparable in both size and molecular weight.

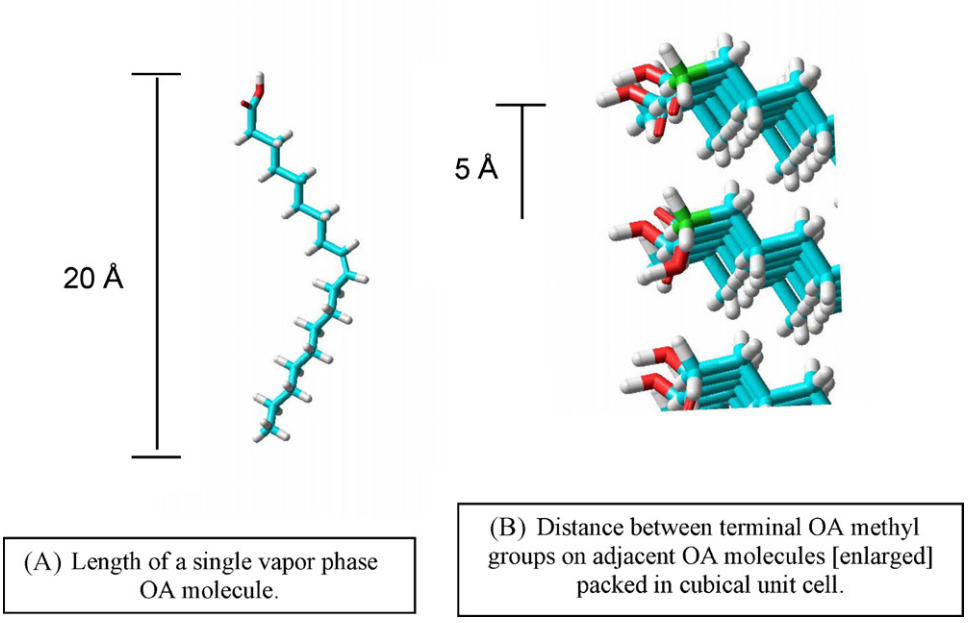


**Fig. 2.** Molecular size and packing spacing of OA using molecular mechanics calculations.

Molecular mechanics calculations predict (1) OA is a wide-angle V (Fig. 2A) and (2) OA packs in unit cells. The closest spacing between carbon atoms on one chain to a neighboring chain by these calculations within the unit cell is 5.0 Å (Fig. 2B) [11% further than 4.5 Å]. The C (chain 1) to H atom (on chain 2) length is 4.2 Å [6.7% closer than 4.5 Å]. In the cubic unit cell, these molecular spacings occur regularly and repeatedly (Fig. 2C). Any irregularly or non-regularity in the alignment of OA molecules would disrupt this molecular distance.

The length across five columns of OA at van der Waals distances from each other equaled 18.16 Å; four molecules within a column at van der Waals distances from each other equaled 16.60 Å. The shortest linear distance in the OA molecule from the initial H on CH3– to the terminal H on –OH was 20.0 Å. Thus, the unit cell volume was 6029 $Å^3$. The cube root of this is 18.2 Å [4.6% larger than X-ray results of 17.4 Å]. One possible explanation is that the wide-angle V is slightly too flat in these models of OA. Another is that cubes are actually more like cylinders, and the conformation of OA in the cylinder could be 4.6% shorter as the aggregate than as the individual molecule.

The major difficulty with assuming non-regularity in packing within a unit cell is that all non-regularity creates an excessively large space in which no lipid is present. The unavoidable question is whether void volume is large or small relative to the size of SA, OA, and MeOA molecules. Regular packing within a cubic unit cell enables the composition of a lipid mixture to exhibit stoichiometry independent of the unpredictably and non-regularity of void volumes. If lipid packing is disorderly, the volume fraction of space between lipids will be large and lipids would be compressible. If lipids pack within a cubic phase, the volume fraction of space between cubic volumes is minimal and even under compression lipid density would remain quite constant.

Raman mapping verified that microscopically, stoichiometry is uniform even if macroscopically, size and shape of structures are variable. In principle, stoichiometry could be uniform on the nanoscale and/or the picoscale level and variable at the molecular level. A difficulty with this hypothesis is that any localized variation in heterogeneity always equals the beginning of two sites of localized homogeneity. Indeed, a phase separation of lipids could be considered the growth of stable sites of localized homogeneity. The boundary conditions of any localized regions would always be discrete or gradually different. In either case, testing alternative hypotheses which contain such non-uniformity require evidence of the size and distribution of the corresponding void volumes.

Twenty OA packed into a cubic volume have wide-angle V groove at the middle of one face of the cube. One SA molecule fits easily within this groove (Fig. 3$A_1$ and $A_2$). The length of a SA is comparable to the width of the five OA molecules in the cube. At a mole ratio of 1/20, SA is 5 mol% of OA. The model supports that at 2% SA, less than half of the unit cells have SA in the groove. Above 5% SA, association between neighboring unit cells could be occurring, resulting in the observed cloudiness. SA sticks out slight beyond the dimensions of the cubic cell, providing a structural basis for perturbing order among neighboring unit cells.

MeOA is structurally the same shape as OA, except it is one $–CH_2–$ group longer, i.e. at the polar terminal end [–OH is $–O–(CH_2)–H$]. Thus, with the same number of 20 molecules of MeOA (5 rows of 4 columns), one SA molecule still fits into the groove of MeOA molecules (not shown) just like with OA. The only difference is that the computed unit cell is a little longer: the SA no longer sticks out from the unit cell. This could explain structurally why at the same concentration, SA in OA is cloudy and why SA in MeOA is fully soluble. In MeOA, the $–R–O–(CH_3)$ region is bulkier than and R–O–H

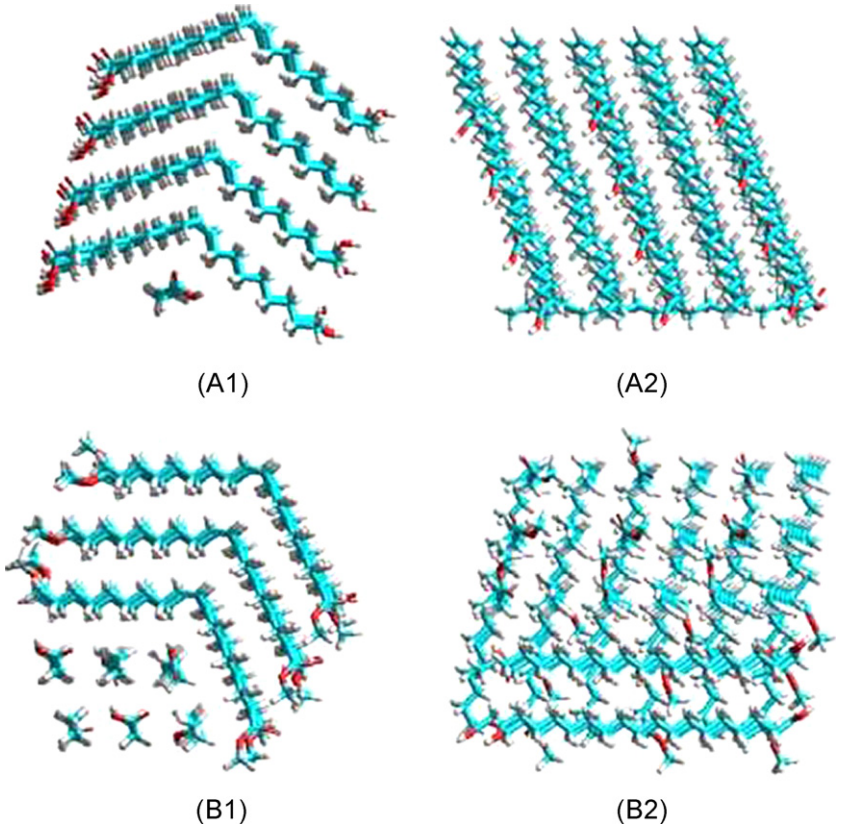


**Fig. 3.** Energy minimized packing of saturated lipid (SA) in mono-unsaturated lipid (OA or MeOA) at stoichiometric mole ratios. (A1) Top view of SA in OA mole ratio 1/20 in cubic phase volume. (A2) Side view of SA in OA mole ration 1/20 in cubiuc phase volume. (B1) Top view of SA in MeOA mole ratio 6/18 (1/3) in cubic phase volume. (B2) Side view of SA in MeOA at mole ratio 6/18 (1/3) in cubic phase volume. Van der Waals forces maintain conformations within unit cells.

and the parallel chain $-CH_2-CH_3$ aligns somewhat closer with the latter than with the former.

A slightly larger unit cell for MeOA has 24 molecules (6 rows of 4 columns). A mole ratio of 1/3 equals 6 rows of SA and 18 rows of MeOA, where 6 of 24 lipids or 25% are SA. Three parallel columns of MeOA have the space for 6 SA to fit parallel to each other and perpendicular to the MeOA molecules (Fig. 3$B_1$ and $B_2$). The shape of the unit cell from the top (Fig. 3$B_1$) is now a hexagon and the net shape of the unit cell approximates a cylinder. Since the axis of the cylinder can as equally be in an X, Y or Z direction, averaged over all three directions, the net effect is a cube with void volume. Molecular dynamics is primarily a function not of the motion of individual molecules, but of aggregates containing discrete numbers of molecules.

The 5% SA in MeOA mixture contains the 21 lipid molecules [20 molecules of MeOA + 1 molecule of SA] molar volume per unit cell. In contrast, the 25% SA in MeOA contains 24 lipid molecules [18 molecules of MeOA + 6 molecules of SA]. In each of the two phases, OA is organized into unit cells and SA stabilizes the size and shape of the unit cells.

A proposed mechanism for formation of the second phase is: (A) An additional SA molecules could migrate into the broad V shaped site forming a unit cell [20 MeOA + 2 SA]; (B) two unit cells [each 20 MeOA + 2 SA] align; (C) 40 MeOA + 4 SA separates into 21 MeOA + 1 SA and 19 MeOA + 3 SA; (C) two aggregates align [19 MeOA + 3 SA and 19 MeOA + 3 SA]; (D) two 19 MeOA + 3 SA align; (E) 38 MeOA + 6 SA separates into 18 MeOA + 5 SA and 20 MeOA + 1 SA; and (F) 20 MeOA + 2 SA plus 18 MeOA + 5 SA rearrange to 18 MeOA + 6 SA plus 20 MeOA + 1 SA . The 24 molecule lipid phase may be immiscible from the 21 molecule lipid phase because the unit cells within each set with discrete stoichiometry are similar in size, shape, dynamics and/or density.

This mechanism proposes that the order of OA and MeOA, not the order of SA, causes the phase separation. Double bonds at the molecular level are always planar, and alignment of double bonds in parallel can be lower energy than perpendicular alignment. Alignment among the double bond region of OA and MeOA appears to order the structure of the unit cell. In saturated solutions of SA in solvent, solvents flow more freely cell-to-cell than SA. In saturated solutions of SA in OA and MeOA, SA would flow more freely cell-to-cell than the unsaturated lipids.

The slow rate of formation of the higher lipid concentration phase could relate to the fact the each step in its formation is reversible. Variable temperatures for example could be the equivalent of turbulence and postpone formation of a uniform second phase. Exchange rates within both phases need to be greater than exchange rates between the two phases. Otherwise, one phase would be constantly increasing in volume and SA in the other phase would become depleted.

## 4. Conclusions

Above a threshold concentration, binary mixtures of SA in OA (and in MeOA) form two immiscible phases and the composition of the resulting phases is stoichiometric. A 5% SA mixture in OA is cloudy; a 5% SA solution is miscible in MeOA and is clear. At 10% SA in MeOA, an immiscible phase formed within a week. The second phase was not 100% SA, nor 10% SA. The immiscible phase had the discrete composition of 25% SA.

Lipid mixtures self-associate into cubical unit cell volumes. Individual lipids have a time averaged conformation at the molecular level that is discrete, i.e. SA is a straight chained molecule, and OA is a flattened V shaped molecule. At the molecular level, packing of individual lipids averaged over a corresponding time must also result in a discrete time averaged conformation. The number of lipid molecules which can pack in any cubic unit cell volumes based upon a shape would also be discrete. Mixtures of lipids pack better within cubic unit cells than structurally identical lipids.

The discreteness in the size and composition within the unit cubic cell volume can be the critical factor in identifying which mixture of lipids are miscible and/or immiscible under any specific conditions. Indeed unless compositions are discrete, all lipids would be fully miscible at any mole ratio with each other and no lipid mixtures would be immiscible. The physical properties of lipids are related to the properties of the aggregate lipid molecules and a 3D cubic unit cell volume contains the size, shape and mole ratios in which lipids aggregates.

## References


Adar, F., Jelicks, L., Naudin, C., Rousseau, S.Y., 2003. Elucidation of the atherosclerotic disease process in apo E and wild type mice by vibrational spectroscopy. SPIE USE 7, 1–9.

Broadhurst, C.L., Schmidt, W.F., Crawford, M.A., Wang, Y., Li, R., 2004. $^{13}C$ Nuclear magnetic resonance spectra of natural undiluted lipids: docosahexaenoic-rich phospholipids and triacylglycerol from fish. J. Agric. Food Chem. 52, 4250–4255.

Baeten, V., Hourant, P., Morales, M.T., Apario, R., 1998. Oil and fat classification by FT-Raman spectroscopy. J. Agric. Food Chem. 46, 2638–2646.

Braun, S., Kalinowski, H.-O., Berger, S., 1998. 150 and More Basic NMR Experiments. Wiley-VCH, Weinheim, p. 250.

Imahara, H., Minami, E., Saka, S., 2006. Thermodynamic study on cloud point of biodiesel with its fatty acid composition. Fuel 85, 1666–1670.

Inoue, T., Hisatsugu, Yamamato, R., Suzuki, M., 2004. Solid–liquid phase behavior of binary fatty acid mixtures. 1. Oleic acid/stearic acid and oleic acid/behenic acid mixtures. Chem. Phys. Lipids 127, 143–152.

Iwahashi, M., Yamaguchi, Y., Kato, T., Horiuchi, T., Sakurai, I., Suzuki, M., 1991. Temperature dependence of molecular conformation and liquid structure of *cis*-9-octadecanoic acid. J. Phys. Chem. 95, 445–451.

Iwahashi, M., Takebayashi, S., Taguchi, M., Kasahara, Y., Minami, H., Matsuzawa, H., 2005. Dynamical dimer structure and liquid structure of fatty acids in their binary liquid mixture: decanoic/octadecanoic acid and decanoic/dodedanoic acid systems. Chem. Phys. Lipids 133, 113–124.

Li, R., Schmidt, W.F., Rankin, S., Walzem, R.L., Boyle-Roden, E., 2003. Solubilization of acylglycerol in phosphatidylcholine vesicles. J. Agric. Food Chem. 51, 477–482.

Schmidt, W.F., Barone, J.R., Francis, B., Reeves III, J.B., 2006. Stearic acid solubility and cubic phase volume. Chem. Phys. Lipids 142, 23–32.

Socrates, G., 2001. Infrared and Raman Characteristic Group Frequencies, Third Edition. John Wiley & Sons, LTD, Chichester, England.

Tomsic, M., Andrej, Jamnik, Gerhard, Fritz-Popovski, Otto, Glatter, Lukas, Vlcek, 2007. Structural properties of pure simple alcohols from ethanol, propanol, butanol, pentanol, to hexanol: comparing Monte Carlo simulations with experimental SAXS data. J. Phys. Chem. B 111, 1738–1751.

Zhdanov, R.I., Dyachkov, E.P., Strazhevskaya, N.B., Dyachkov, P.N., 2003. DNA -bound lipids: computer modeling of DNA interaction with stearic acid and unsaturated fatty acids. Russ. Chem b Bulletin Chem. Bull. 52, 1893–1899.